Isotropic NMR Spectra of Half-Integer Quadrupolar Nuclei Using Satellite Transitions and Magic-Angle Spinning

Zhehong Gan*

Center of Interdisciplinary Magnetic Resonance
National High Magnetic Field Laboratory
1800 East Paul Dirac Drive, Tallahassee, Florida 32310

Received November 12, 1999
Revised Manuscript Received February 18, 2000

Nuclear magnetic resonance (NMR) spectroscopy has become an important tool for structural characterization of many important materials such as minerals, ceramics, glasses, semiconductors, and catalysts which contain elements such as ^{11}B, ^{17}O, ^{23}Na, ^{27}Al, ^{71}Ga, and ^{87}Rb.[1] NMR spectra of nuclei with spin $S > {}^1/_2$ are dominated by the nuclear quadrupolar spin interaction. For half-integer quadrupolar nuclei, relatively narrow spectral lines can be obtained by limiting observation only to the central ${}^1/_2 \leftrightarrow -{}^1/_2$ NMR transition for which the first-order quadrupolar effect vanishes. The second-order quadrupolar effect contains high-rank anisotropic terms which are not completely averaged by magic-angle sample spinning (MAS).[2] Although high magnetic fields can reduce the second-order effect, a complete removal of line broadening requires double rotation (DOR)[3] or dynamic angle spinning (DAS)[4] to achieve isotropic spectra. Recently, Frydman and Harwood have introduced an elegant method which utilizes multiple-quantum transitions.[5] The multiple-quantum magic-angle spinning (MQMAS) method requires only conventional MAS to obtain isotropic spectra of half-integer quadrupolar nuclei. The sensitivity and the quantitative features of MQMAS largely depend on the efficiency of multiple-quantum excitation and the quest for high efficiency drives an ongoing effort for pulse sequence optimization.[6] In this contribution, a different approach based on satellite transitions is proposed. The satellite transitions in the spin manifold of quadrupolar nuclei can be efficiently excited using short radio frequency pulses and directly observed under MAS.[7] Therefore, as will be shown here the satellite transition MAS method generates isotropic spectra of half-integer quadrupolar nuclei with high efficiencies.

At high magnetic fields, the first- and second-order quadrupolar effects to spin states $-S \le m_S \le S$ can be expanded in terms of spherical harmonics

$$E^{Q(1)}_{S,m_S} = -\omega_Q[S(S+1) - 3m_S^2] \sum_{m=-2}^{m} a^{(1)}_{2,m} Y_{2,m}(\theta,\phi)$$

$$E^{Q(2)}_{S,m_S} = (\omega_Q^2/\omega_L) \sum_{l=0,\,2,\,4} C_l(S,m_S) \sum_{m=-l}^{l} a^{(2)}_{l,m} Y_{l,m}(\theta,\phi) \quad (1)$$

where $\omega_Q = e^2qQ/2S(2S-1)\hbar$ and ω_L is the Lamor frequency, $a^{(1)}_{2,m}$ and $a^{(2)}_{l,m}$ depend only on the asymmetry factor of the electrical field gradient (EFG) tensor, and (θ,ϕ) are the polar angles of the magnetic field in the principal axis frame of the EFG tensor. The first-order terms $E^{Q(1)}_{S,m_S}$ have no effect on the ${}^1/_2 \leftrightarrow -{}^1/_2$ central transition as $E^{Q(1)}_{S,1/2} = E^{Q(1)}_{S,-1/2}$. For satellite transitions, the first-order effect can be averaged by MAS as it contains only the second-rank anisotropic term, $Y_{2,m}(\theta,\phi)$. The second-order effect $E^{Q(2)}_{S,m_S}$ contains the isotropic $l = 0$ and the anisotropic $l = 2, 4$ terms with the expansion coefficients

$$C_l(S, m_S) = C(22l, 1-1)[4S(S+1) - 8m_S^2 - 1]m_S$$

$$+ C(22l, 2-2)[2S(S+1) - 2m_S^2 - 1]m_S \quad (2)$$

where $C(22l, 1-1)$ and $C(22l, 2-2)$ are the Clebsh−Gordon coefficients. The ratios between the ${}^{\pm 3}/_2 \leftrightarrow {}^{\pm 1}/_2$ and the central transition frequencies for $l = 0, 2, 4$ are listed in Table 1.[8] Under MAS, the second-rank $l = 2$ terms are averaged, but the high-rank $l = 4$ terms are only scaled by $P_4(\cos\theta_M)$ which causes broadening to both the central transition lines and the spinning sidebands from satellite transitions as shown in Figure 1. The remaining broadening can be completely removed by a correlation between the satellite and central transitions in a two-dimensional (2D) experiment. As listed in Table 1, the $l = 4$ terms between the satellite and central transitions are different only by a scaling factor, R. Thus the dephasing of time-domain signals is refocused at $t_2 = RT_1$ and the refocusing leads to an averaging of the remaining $l = 4$ terms for isotropic spectra.

The correlation between satellite and central transitions can be established using a two-pulse sequence where the first pulse excites satellite transitions and the second pulse transfers coherence to the central transition. A three-pulse version with a z-filter replacing the second pulse permits the data acquisition in hypercomplexform for pure absorptive spectra. Figure 2 demonstrates the satellite transition MAS experiment using a mixture of $^{23}Na_2SO_4$ and $^{23}Na_2C_2O_4$ as a model system. The correlation of satellite transitions along F_1 and the central transition along F_2 yields ridge-shaped peaks parallel to each other. The slope of the ridges equals to the ratio in Table 1 for $l = 4$ and is $-8/9$ for ^{23}Na spins. A spectral tilt along F_1 yields an isotropic-anisotropic 2D spectrum where the projection along F_1 is not affected by the second-order quadrupolar interaction. The resulting isotropic peak position in F_1 can be derived from the ratios in Table 1 for $l = 0$ of $S = {}^3/_2$ spins

$$\omega_{iso} = \frac{17}{9}\omega_\delta - \frac{10}{9}\omega_0^{(2)} \quad (3)$$

where ω_δ is the isotropic chemical shift frequency and

* Author for correspondence. Telephone: (850) 644−4662. Fax: (850) 644−1366. E-mail: gan@magnet.fsu.edu.

(1) (a) Maciel, G. E. *Science* **1984**, *226*, 282. (b) Oldfield. E.; Kirkpatrick, R. J. *Science* **1985**, *227*, 1537.

(2) (a) Kundla, E.; Samoson, A.; Lippmaa, E. *Chem. Phys. Lett.* **1981**, *83*, 229. (b) Ganapathy, S;. Schramm, S.; Oldfield, E. *J. Chem. Phys.* **1982**, *77*, 4360. (c) Lefebvre, F.; Amoureux, J. P.; Fernandez, C.; Deronane, E. G. *J. Chem. Phys.* **1987**, *86*, 6070.

(3) (a) Samoson, A.; Lippmaa, E.; Pines, A. *Mol. Phys.* **1988**, *65*, 1013. (b) Chmelka, B. F.; Mueller, K. T.; Pines, A.; Stebbins, J.; Wu, Y.; and Zwanziger, J. W. *Nature* **1989**, *339*, 42.

(4) (a) Llor, A.; Virlet, J. *Chem. Phys. Lett.* **1988**, *152*, 248. (b) Mueller, K. T.; Sun, B. Q.; Chingas, G. C.; Zwanziger, J. W.; Terao, T.; Pines, A. *J. Magn. Reson.* **1990**, *86*, 470. (c) Farnan, I.; Grandinetti, P. J.; Baltisberger, J. H.; Stebbins, J. F.; Werner, U.; Eastman, M. A.; Pines; A. *Nature* **1992**, *358*, 31.

(5) (a) Frydman, L.; Harwood: J. S. *J. Am. Chem. Soc.* **1995**, *117*, 5367. (b) Medek, A.; Harwood: J. S.; Frydman, L. *J. Am. Chem. Soc*. **1995**, *117*, 12779.

(6) (a) Fernandez, C.; Amoureux, J. P. *Chem. Phys. Lett.* **1995**, *242*, 449. (b) Wu, G.; Rovnyank, D.; Sun, B.; Griffin, R. G. *Chem. Phys. Lett*. **1996**, *249*, 210. (c) Wu, G.; Rovnyank, D.; Griffin, R. G. *J. Am. Chem, Soc.* **1996**, *118*, 9326. (d) Massiot, D.; Tonzo, B., Trumeau, D.; Coutures, J. P.; Virlet, J.; Florian, P.; Grandinetti, P. J. *Solid State Nucl. Magn. Reson.* **1996**, *6*, 73. (e) Duer, M. J.; Stourton C. *J. Magn. Reson.* **1997**, *124*, 189. (f) Fernandez, C.; Amoureux, J. P. *Solid State Nucl. Magn. Reson.* **1998**, *10*, 211. (g) Amoureux, J. P.; Fernandez, C.; Steuernagel, S. *J. Magn. Reson. A* **1996**, *119*, 280. (h) Brown, S. P.; Heyes, S. J.; Wimperis, S. *J. Magn. Reson. A* **1996**, *119*, 280. (i) Massiot, D. *J. Magn. Reson. A* **1996**, *122*, 240. (j) Ding, S.; McDowell, C. A. *Chem. Phys. Lett.* **1997**, *270*, 81. (k) Marinelli, L.; Medek, A.; Frydman, L. *J. Magn. Reson.* **1998**, 132, 88. (l) Ding, S.; McDowell, C. A. *J. Magn. Reson.* **1998**, *135*, 61.

(7) Jakobsen, H. J., Skibsted, J., Bildsøe, H., Nelsen, N. C., *J. Magn. Reson.* **1989**, *85*, 173.

(8) Rose, M. E., *Elementary Theory of Angular Momentum*; Wiley: New York, 1961.

10.1021/ja9939791 CCC: $19.00
Published on Web 03/16/2000

Table 1. Ratios of $l = 0$, 2, 4 Expansion Coefficients between $+1/2 \leftrightarrow +3/2$ and the Central Transitions for Spins $S = 3/2$, $5/2$ and $7/2$

	rank $l = 0$	2	4
$S = 3/2$	−2	−1/2	−8/9
$5/2$	−1/8	7/16	7/24
$7/2$	1/10	7/10	28/45

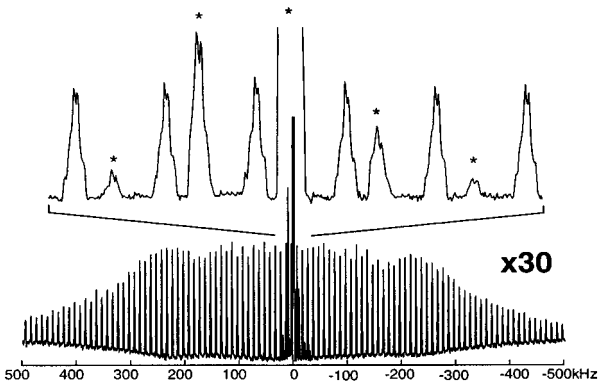

Figure 1. ^{23}Na magic-angle spinning spectrum of Na_2SO_4 showing the spinning sidebands of the $\pm 3/2 \leftrightarrow \pm 1/2$ transitions and the central transition lines (*).

$$\omega_0^{(2)} = \frac{[S(S+1) - 3/4]\omega_Q^2}{[2S(2S-1)]^2\omega_L}\frac{3}{10}\left(1 + \frac{1}{3}\eta^2\right)$$

is the isotropic part of the second-order quadrupolar effect.

The complete averaging of the first-order quadrupolar effect is critical for the satellite transition MAS experiment which requires the spinning axis to be precisely on the magic-angle. Also the evolution time t_1 needs be a multiple of the rotor period. A dwell time fixed to the rotor period causes a folding of spinning sidebands into the spectral window that equals the rotor frequency. The constructive superposition of all spinning sidebands yields a total spectral intensity close to that for the central transition line, although the intensity of an individual spinning sideband is very low. Besides setting the magic-angle and evolution time t_1, the satellite transition MAS experiment requires short radio frequency pulses to cover the wide spectral width of the satellite transitions. The pulse length, experimentally optimized for the sample in Figure 2, is about 31° and 36° in terms of flip angle for the excitation and the coherence transfer of satellite transitions.

The relative sign of the $l = 4$ terms between the satellite and central transitions determines the coherence transfer pathway for the satellite transition MAS experiment. For $S = 3/2$ spins, the $p = -1(t_1) \rightarrow -1(t_2)$ pathway leads to an *echo* for cross-peaks between the satellite and central transitions, but only an *antiecho* for diagonal peaks of the central transitions. The diagonal peaks can be further reduced by applying a soft pulse prior to the pulse sequence. Saturation of the central transition can also increase the polarization of satellite transitions.[9] The three-pulse sequence selects both the $p = -1 \rightarrow -1$ and the $+1 \rightarrow -1$ pathways. Thus the resulting 2D spectrum shows both the cross and diagonal peaks which have opposite signs. Considering that the central transition is not affected by the frequency offset from the first-order quadrupolar effect, the intensity ratio between the cross and diagonal peaks is a good indicator on the efficiency of satellite transition MAS experiment. The projections in Figure 2d show a ratio of about 0.3 for the three-pulse sequence and about 0.8 for the two-pulse sequence, both with an rf field strength $\gamma B_1/2\pi$ of 50 kHz.

(9) (a) Hasse, J., Conradi, M. S., *Chem. Phys. Lett.* **1993**, *209*, 287. (b) Kentgens, A. P. M.; Verhagen, R., *Chem. Phys. Lett.* **1999**, *300*, 453.

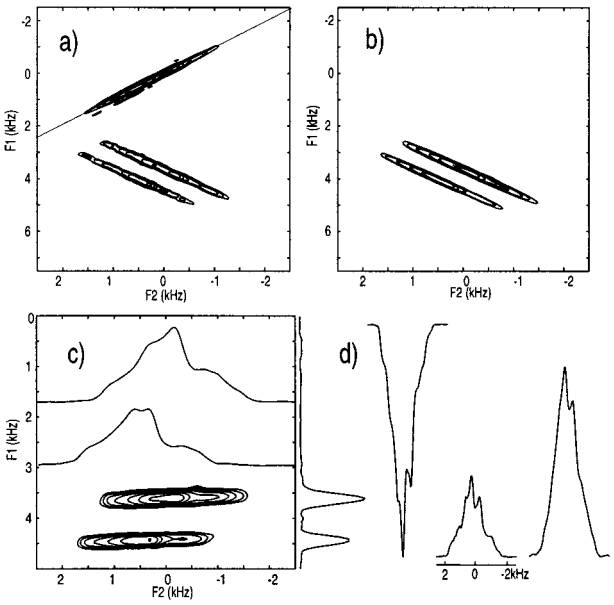

Figure 2. Figure 2. 2D satellite transition MAS spectra of a mixture of Na_2SO_4 and $Na_2C_2O_4$. (a) acquired using the p_1-t_1-p_2-τ-p_3-t_2 three-pulse sequence. (b) using the p_1-t_1-p_2-t_2 two-pulse sequence. (c) 2D spectrum obtained by a spectral tilt (b) along with the isotropic spectrum projected in F_1 and F_2 slices of the two ^{23}Na peaks. (d) F_2 projections (from left to right) of the diagonal peak in (a), cross-peaks in (a), and cross-peaks in (b) displayed on an absolute scale for comparison of sensitivity. In (a), the hypercomplex 2D data were acquired using $\phi_1 = x\ -x$; $\phi_2 = x$ for real ($-y$ for imaginary); $\phi_3 = x\ x\ -x\ -x$; and $\phi_{rec} = x\ -x\ -x\ x$ phase cycle. The pulse lengths p_1, p_2, and p_3 were experimentally optimized to 1.75, 1.75, and 2 μs, with $\gamma B_1/2\pi = 50$ kHz. A total of 64 (32 complex) t_1 increments with 100 μs per step and 4 acquisitions per increment were acquired in 256 s. The first t_1 increment started at 98.5 μs, considering the finite pulse lengths of p_1 and p_2. A *diagonal* line was drawn in the 2D plot with nonequal spectral widths. In b), the $p \rightarrow -1 \rightarrow -1$ coherence transfer pathway was selected using the phase cycle, $\phi_1 = x\ -x$; $\phi_2 = x\ x\ y\ y$; and $\phi_{rec} = x\ -x$. The pulse lengths p_1 and p_2 were experimentally optimized to 1.75 and 2 μs. A 40 μs soft pulse with $\gamma B_1/2\pi = 5$ kHz was applied to saturate the central transition prior to the pulse sequence. A total of 32 t_1 increments with 4 acquisitions per increment were acquired in 128 s. All experiments were performed on a 600 MHz (^{1}H) wide bore magnet using a Bruker DMX console equipped with a 4 mm MAS probe. The spinning frequency was regulated at 10 kHz within ±2Hz. The magic-angle was set by maximizing the rotational echo in the ^{23}Na free-induction decay of a $NaNO_3$ sample and a Bruker sample changer was used to eject and to load sample rotors without taking the probe out of the magnet.

It has been shown that the correlation between satellite and central transitions can be obtained efficiently using simple pulse sequences for achieving isotropic spectra of half-integer quadrupolar nuclei under magic-angle sample spinning. The strict requirement for setting the magic-angle accurately can be easily satisfied using current state-of-art NMR hardware. The advantage of high spectral resolution and sensitivity along with the information available on EFG tensors make the satellite transition MAS method a very useful NMR experiment especially at high magnetic fields for the study of solid materials containing half-integer quadrupolar nuclei.

Acknowledgment. This work is supported by the National High Magnetic Field Laboratory through the NSF Cooperative Agreement DMR-9527035 and by the State of Florida.

JA9939791